Int. J. Electrochem. Sci., 15 **(2020)** 8808 – 8822, doi: 10.20964/2020.09.82

International Journal of
ELECTROCHEMICAL
SCIENCE
www.electrochemsci.org

Fabrication of Gold nanoparticles/Carbon Quantum Dots Nanocomposites for the Electrochemical Analysis of Ascorbic Acid, Dopamine and Uric Acid

Yuyun Wei[1, †], *Zhifang Xu*[1, †], *Di Zhang*[2,*] , *Yuxin Fang*[1,*]

[1] Research Center of Experimental Acupuncture Science, College of Acumox and Tuina, Tianjin University of Traditional Chinese Medicine, Tianjin 301617, PR China
[2] College of Pharmaceutical Engineering of Traditional Chinese Medicine, Tianjin University of Traditional Chinese Medicine, Tianjin 301617, PR China
[*]E-mail: 43987073@qq.com (D. Zhang), meng99_2006@126.com (Y.X. Fang)
[†]These authors contributed equally.

Received: 1 June 2020 / *Accepted:* 10 July 2020 / *Published:* 10 August 2020

A sensitive and straightforward sensor consisting of a glassy carbon electrode (GCE) containing carbon quantum dots (CQDs), and gold nanoparticles (AuNPs), was fabricated for simultaneous detection of ascorbic acid (AA), dopamine (DA) as well as uric acid (UA). Composite AuNPs/CQDs/GCE and its components were examined using high-resolution transmission and field emission scanning electron microscopies (HRTEM and FESEM, respectively), energy-dispersive and electrochemical impedance (spectroscopies EDS and EIS, respectively), as well as cyclic voltammetry (CV). The synergetic effect, of AuNPs and CQDs provided GCE with an outstanding electrocatalytic rate and excellent selectivity towards AA, DA, and UA oxidation in 0.1M PBS. The linear response ranges of the electrodes were 300-700 and 800-3500 μM for AA, 2-32 μM for DA, and 30-100 and 120-200 μM for UA. The peak potential separation values (ΔE_p) of AA-DA, DA-UA, and AA-UA pairs were equal to 150, 130, and 280 mV, respectively. The sensitivity of AuNPs/CQDs/GCE was 0.012 and 0.0057 μA/μM towards AA, 405.13 μA/μM towards DA, as well as 0.148 and 0.044 μA/μM towards UA. Our electrochemical sensor showed excellent stability, analysis reproducibility, and repeatability.

Keywords: Carbon quantum dots; Au nanoparticles; Ascorbic acid; Dopamine; Uric acid

1. INTRODUCTION

A variety of bio-active and bio-important molecules coexisting in biological matrices and playing critical roles in physiology and functioning of living things is enormous. Recent progress in medicine and diagnostics includes the detection of physiological indicators in biological samples, which is attracting a lot of attention from scientists and doctors worldwide [1]. A variety of practical state-of-the-

art analytical methods for biological sample analyses and simultaneous detection of their multiple components was recently reported. One such method is an electrochemical one, which also offers ease of operation and fast response together with high sensitivity and selectivity. In combination with its low cost, excellent reproducibility and accuracy, electrochemical detection of biomolecules in physiological samples might soon be a dominating analytical technique. [2-4].

Dopamine (DA) is vital for numerous physiological processes, including brain functioning, emotional and motivational controls as well as endocrine gland regulations. It is also an essential part of the cardiovascular and nervous systems [6]. Because DA participates in electrical signal transfer from the brain to other body parts and organs, its abnormal levels often cause neurological disorders from Parkinson's disease to schizophrenia [7-9]. Ascorbic acid (AA) is also a pivotal substance to maintain normal physiological functions of our bodies [10]. It inhibits cancer, fights, or even cures a common cold as well as improves mental health [11, 12]. Uric acid (UA) is present in blood and urine, and its levels often indicate certain disorders and illnesses, including gout, Lesch-Nyhan syndrome, hyperuricemia, etc [13, 14]. Thus, the presence and levels of DA, UA and AA in bio-systems need to be analyzed. However, the simultaneous electrochemical analysis of AA, DA, and UA is somewhat difficult because their oxidation potentials are close, which often makes their voltammetric peaks indistinguishable [15, 16]. Thus, the sensor capable of overcoming the mutual interference of these substances is needed.

Carbon quantum dots (CQDs) are nanoparticles with sizes below 10 nm. CQDs, obtained during purification of electrophoretically synthesized single-walled carbon nanotubes, were mentioned for the first time in 2004 [17, 18]. CQDs are soluble in water but still chemically inert. In addition, it is extremely easy to functionalize them. Their other outstanding properties (including high resistance to photobleaching, low toxicity, excellent biocompatibility, and electron acceptor/electron donor ability) make them very promising for a variety of applications related to bioimaging, photocatalysis, nanomedicine, and other fields [19-26]. CQDs are also very suitable as active materials for electrochemical (bio)sensors [27-32]. Their electrochemical activity can be improved even further by combining them with other nanoparticles (NPs). Among various metal NPs, gold NPs (AuNPs) are also biocompatible and non-toxic, as well as quite easy to disperse. These and other unique properties made them popular catalysts for applications related to biomedical, biotechnological, and sensing fields [33, 34]. Several groups recently published research data on fluorescence sensors for DA, AA and UA determination based CQDs and Au nanomaterials [35, 36]. However, relevant research on electrochemical sensors is still lacking.

Therefore, this work reports a simple and easy method to modify the glassy carbon electrode (GCE) by two-step electrodeposition using a composite material containing both CQDs and Au NPs. The presence of CQDs offered higher surface area, while AuNPs interaction with CQDs provided faster electron transfer. Because of the synergetic effect of CQDs and AuNPs coexistence in the composite GCE, the resulting AuNPs/CQDs/GCE-based sensor was able to split electrochemical oxidation peaks of AA, DA and UA and demonstrate low detection limit as well as excellent sensitivity and selectivity.

2. EXPERIMENTAL

2.1. Initial materials and chemicals

Ascorbic acid (AA) was obtained from Lianxing Biotechnology. Dopamine (DA) hydrochloride was acquired from Sigma-Aldrich. Polyethylene glycol with molecular weight equal to 200 was obtained from Beijing Solarbio Science & Technology. Uric acid (UA) was supplied by the Ron Chemical Reagent Company. Chloroauric acid ($HAuCl_4$) was purchased from Shanghai Yuanye Biotechnology Co. Potassium chloride（KCl）and glucose were from the Tianjin Chemical Reagent Factory. 0.1 M phosphate buffer solution (PBS) with pH = 7.0 was prepared from the corresponding ratios of Na_2HPO_4 and NaH_2PO_4. All solutions were prepared using ultrapure water. All chemicals were used as received. Unless mentioned otherwise, all experiments were performed at pH = 7.0.

2.2. Instrumental characterization and tests

All electrochemical tests (cyclic and differential pulse voltammetry, CV and DPV, respectively, as well as electrochemical impedance spectroscopy, EIS) were performed using AMETEK PARSTAT 4000 workstation and a three-electrode setup, in which GCE, saturated calomel electrode (SCE) and Pt acted as working, reference and counter electrodes, respectively. DPV tests were conducted in PBS in the -1.5 - 1.5 V sweeping potential range using 0.2 s pulse width and 50 mV amplitude. CV and EIS were performed in 0.1 M KCl containing 20 mM $[Fe(CN)_6]^{3-/4-}$.

Field emission scanning electron microscopy (FESEM) was conducted by a Nova NanoSEM 430 instrument. High-resolution electron microscopy (HRTEM) coupled with the energy dispersive spectroscopy (EDS) was performed using the FEI Talos F200X instrument.

Other equipment used in this work was LX400 centrifuge manufactured by Kylin-Bell Lab Instruments, an LG Electronics microwave, and dialysis tubing (with a 100-500 Da maximum molecular weight cutoff) purchased from Beijing Solarbio Science & Technology.

2.3. CQDs Synthesis

CQDs were synthesized by a one-step process (which involved heating in a microwave) reported elsewhere [37] and modified in our previous work [38]. For this purpose, 20 ml of polyethylene glycol was mixed with 4 g of glucose and 6 ml of water. After the resulting mixture was stirred until it became clear, it was microwaved for 3 min. The resulting dark viscous solution was placed into a dialysis tubing for 24 hours (against water), after which the solution inside the dialysis hose was centrifuged at 6000 rpm for 15 min. The mother solution (which was CQD solution) was separated from the solid product and then stored at 4 °C.

2.4. Preparation of AuNPs/CQDs/GCE

GCE was polished using 0.05 μm alumina slurry placed into a CQDs solution and then subjected to 20 CV cycles (from -1 to 2 V) at 50 mV/s sweeping rate. The resulting CQDs-modified GCE was soaked in 20 mL of 0.1 M KCl containing 1 mM of $HAuCl_4$ at a constant -300 mV potential for 250 s to form AuNPs/CQDs-modified GCE (Au NPs/CQDs/GCE).

3. RESULTS AND DISCUSSION

3.1. Morphology of AuNPs/CQDs composites

As synthesized CQDs were well-dispersed and had an average diameter of ~5 nm (see Fig. 1A). HRTEM analysis of a single CQDs showed crystalline structure with lattice fringes 0.14 nm apart (the details were in the preliminary work of our research group [38]), which were ascribed to the (102) plane of sp^2-hybridized carbon.

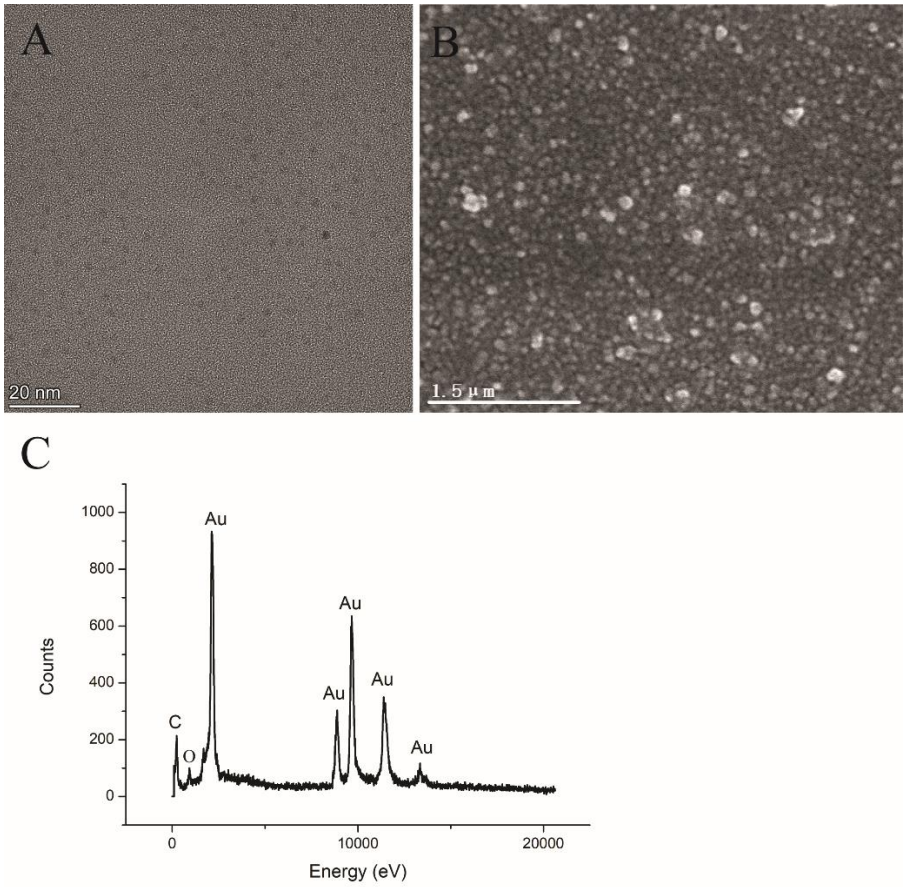

Figure 1. HRTEM micrograph of CQDs (A), FESEM micrograph (B) and EDS data (C) for AuNPs/CQDs composites.

AuNPs electrodeposited onto the CQDs-modified GCE were also well-dispersed (Fig. 1B) mostly because of the stabilizing effect of the CQDs presence, which prevented AuNPs aggregation

during electrodeposition. The AuNPs were spherical with an average diameter of ~35 nm. After AuNPs were deposited on the electrode, the CQDs became rougher (see Fig. 1B), which is also beneficial for electrochemical sensing. EDS data showed C and Au presence on the GCE surface (see Fig. 1C), confirming the successful preparation of an AuNPs/CQDs-modified GCE.

3.2. Electrochemical behavior of different electrodes towards AA, DA, and UA

The electrochemical properties of bare, CQDs- and AuNPs/CQDs- modified GCEs were tested by CV and EIS using 20mM $[Fe(CN)_6]^{3-/4-}$ solution containing 0.1M KCl. CV showed that redox peaks of AuNPs/CQDs modified GCE were significantly higher (see Fig. 2A-c) than analogous peaks of bare and CQDs-modified GCEs (see Fig. 2A-a, b) very likely because modification with AuNPs/CQDs composite enlarged the electrode surface area and accelerated the electron transfer, both of which enhanced the electrode current response. The peak-to-peak potential (ΔEp) between the anodic and cathodic peaks for the AuNPs/CQDs/GCE was lower than for the other two electrodes. Thus, the fast and quasi-reversible electron-transfer process occurred on the surface of AuNPs/CQDs-modified GCE, which is indicative of a favorable microenvironment for the quick electron-transfer reactions. EIS data showed that charge transfer resistance (R_{ct}) of AuNPs/CQDs/GCE was 300 Ω, which is significantly lower than R_{ct} of pristine and CQDs-modified GCE (which were equal to 3000 and 500 Ω, respectively, see Fig. 2B). Such excellent behavior confirmed the results obtained from the EIS tests on excellent electron transfer kinetics of the composite AuNPs/CQDs/GCE as well as its excellent conductivity. Such excellent performance was attributed to the large surface area of that AuNPs/CQDs/GCE, which promoted the electron transfer between the electrode and an analyte.

Fig. 2C demonstrates DPV curves of bare, CQDs- and AuNPs/CQDs- modified GCEs recorded in 0.1M PBS containing a mixture of 0.5 mM AA, 2 μM DA, and 0.1 mM UA. DPV curve of the bare GCE (a) showed barely distinguishable oxidation peaks of AA and DA (see a relatively broad peak at 0.15 V). Thus, bare GCE cannot simultaneously detect AA and DA. Electrooxidation peak current and separation of the peak potentials observed for the AuNPs/CQDs/GCE (which were equal to 150, 130 and 280 mV for AA-DA, DA-UA, and AA-UA, respectively) were larger than those observed for CQDs/GCE. Thus, AuNPs increased the electron transfer rate of the composite AuNPs/CQDs/GCE, which significantly improved the peak current and potential separation of the analytes. These results demonstrated the high electrocatalytic capability of AuNPs/CQDs/GCE of distinguishing AA, DA, and UA.

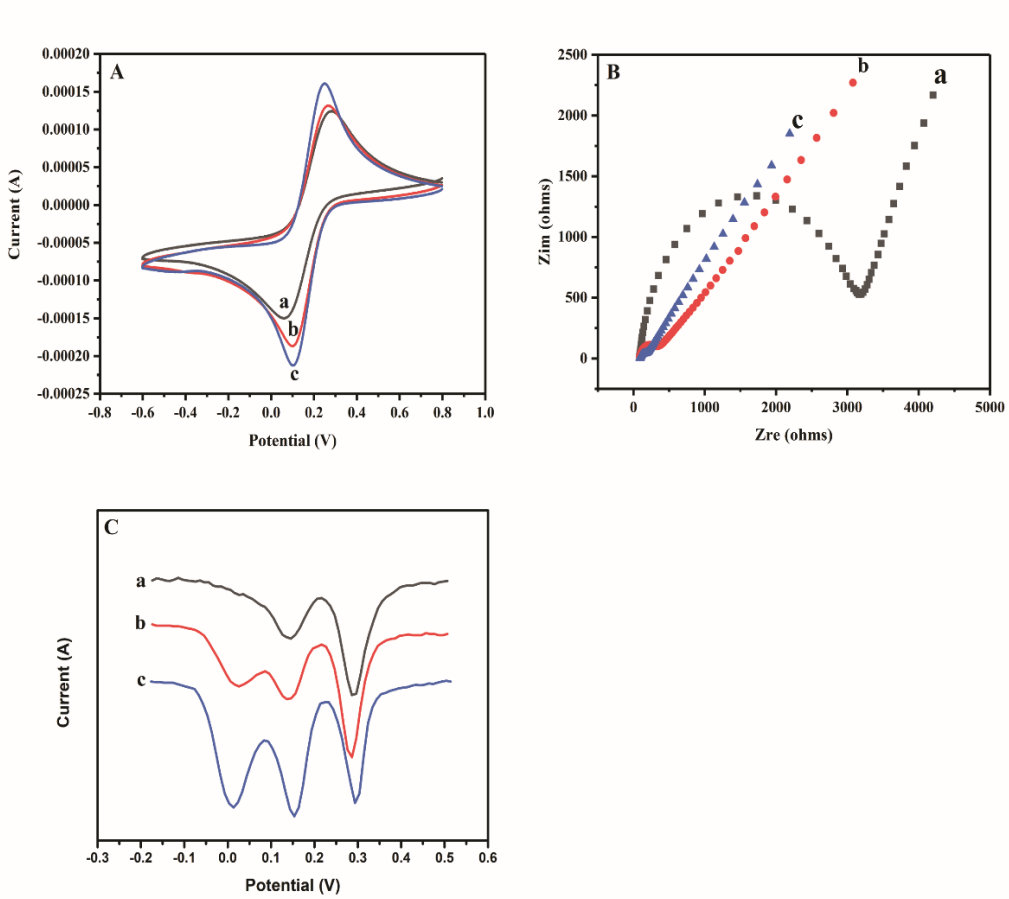

Figure 2. CVs (A) and EIS (B) of bare GCE (a), CQDs/GCE (b), AuNPs/CQDs/GCE (c) in $[Fe(CN)_6]^{3-/4-}$. (C) DPV curves of (a) bare GCE, (b) CQDs/GCE and (c) AuNPs/CQDs/GCE in 0.5 mM AA, 2 μM DA and 0.1 mM UA.

3.3. Influence of pH and scan rate on AuNPs/CQDs/GCE performance during simultaneous AA, DA and UA detection

Typically, an interaction between an analyte and AuNPs/CQDs/GCE strongly depends on the pH. Therefore, we performed simultaneous AA, DA, and UA detection at pH = 5.8-8.0 using DPV (see Fig. 3). The maximum oxidation peak current of the AuNPs/CQDs/GCE under the presence of individual analytes was observed at pH equal to 7.0, 7.2, and 7.0, respectively (see Fig. 3A). The highest peak potential separation for AA-DA and DA-UA was obtained at pH = 7 (see Fig. 3B). Thus, this pH value was chosen for all further detection tests. Additionally, as the solution pH increased, AA, DA, and UA oxidation potentials negatively shifted very likely because of higher proton activity and participation in the electrochemical oxidation reaction, which probably occurred through the electron transfer step followed by protonation of the analyte molecules [39].

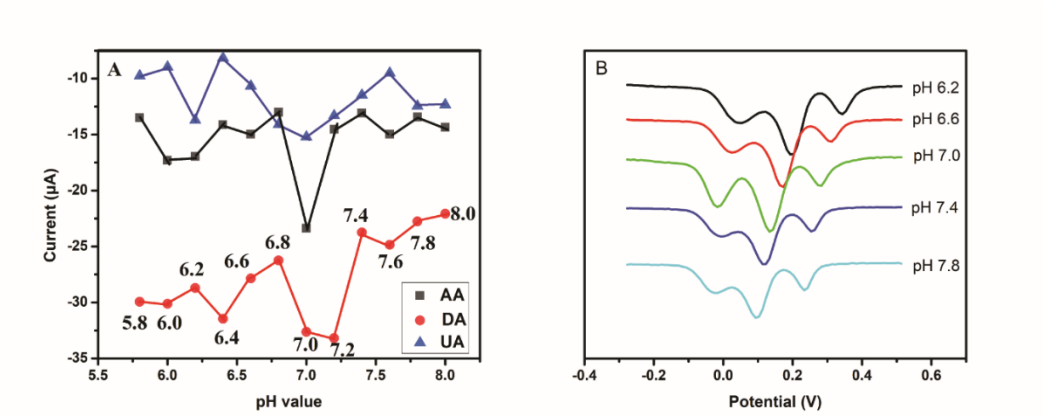

Figure 3. Effect of solution pH on the peak current (A) and potential (B) of simultaneously present AA, DA, and UA.

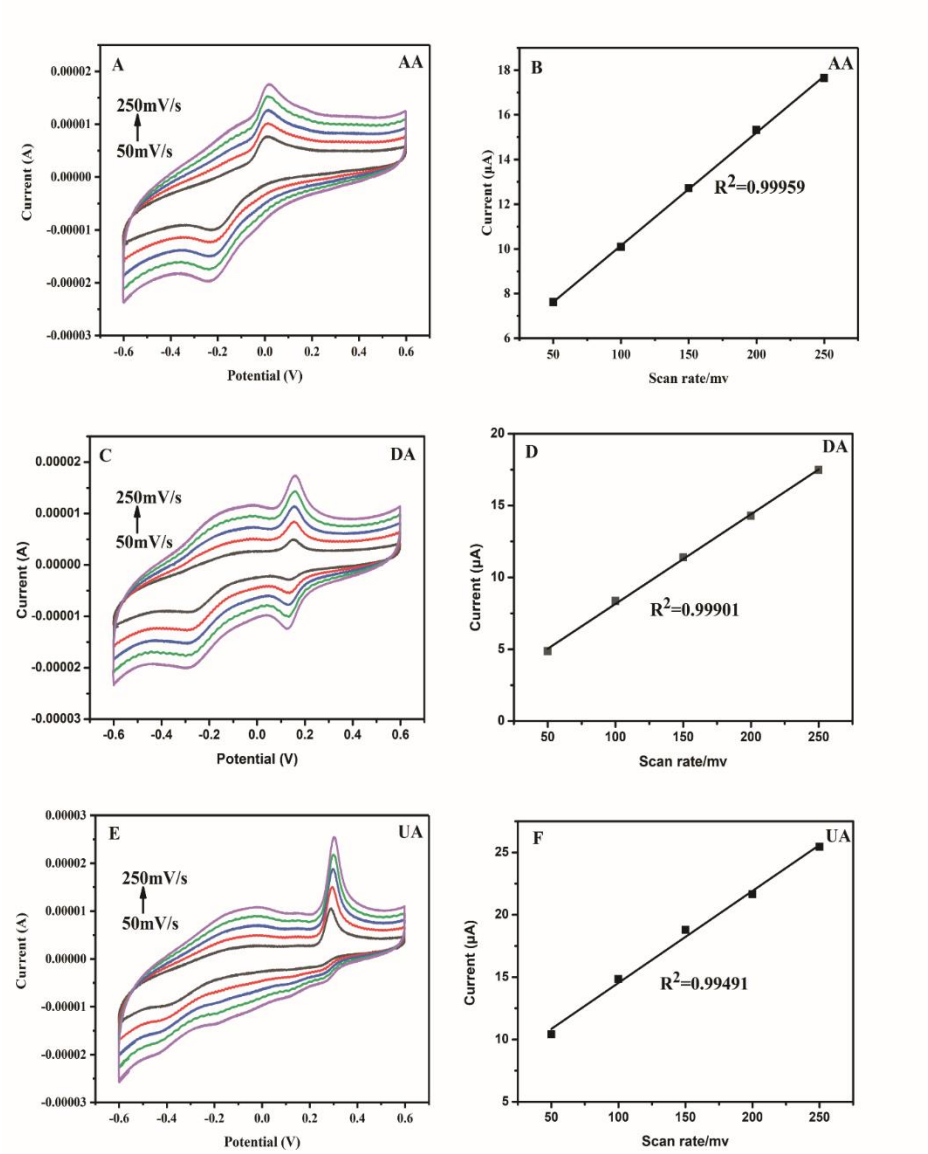

Figure 4. CV curves of AuNPs/CQDs/GCE recorded at 50-250 mV s^{-1} scan rates in 0.1 M PBS at pH equal to 7.0 for the solutions containing (A) 1 mM AA, (C) 15 μM DA and (E) 0.5 mM UA. The corresponding anodic peak current (I_{pa}) values fitted as a function of the scan rate are shown in B, D, and F, respectively.

The influence of the CV scan rate on AuNPs/CQDs/GCE performance regarding 1 mM AA, 15 μM DA, and 0.5 mM UA is shown in Fig. 4. Well-defined AA, DA, and UA anodic oxidation peaks appeared at 0.02, 0.16, and 0.3 V, respectively (see Fig. 4A, 4C, and 4E). The current magnitudes of these peaks were enhanced linearly. The anodic peak potentials shifted positively as the scan rate was increased from 50 to 250 mV s^{-1}. The linear relationships between the current (I_{pa}) and the scan rate for AA, DA, and UA, as well as their corresponding correlation coefficients (R^2), were as follows:

AA: I_{pa}= 5.095+0.051V (mV s^{-1}) (R^2=0.999), see Fig. 3B,

DA: I_{pa}= 1.922+0.062V (mV s^{-1}) (R^2=0.999), see Fig. 3D,

UA: I_{pa}= 7.161+0.074V (mV s^{-1}) (R^2=0.995), see Fig. 3F,

Excellent linear correlation between I_{pa} and the scan rate indicates adsorption-controlled mechanisms of the reaction between AA, DA, and UA and AuNPs/CQDs/GCE surface [40, 41].

3.4. Individual and simultaneous detection of AA, DA, and UA

To demonstrate the applicability of our composite electrodes to detect AA, DA, and UA individually and simultaneously, we used differential pulse voltammetry (DPV), which is a very popular method of electrochemical analysis. AA, DA, and UA detection were performed in the 0.01-10 mM, 1-67 μM, and 0.05-3 mM concentration ranges (see Fig. 5A, C, and E), respectively. The peak currents increased as AA, DA, and UA contents increased, which demonstrated efficient electrochemical oxidation ability of our composite AuNPs/CQDs/GCE as well as the absence of fouling effects [42, 43]. The detection limits were determined using corresponding calibration curves (see Fig. 5B, D, and F) were 3.33, 0.33, and 16.67 μM (S/N = 3), respectively. The linearity ranges for the detection of individual AA, DA, and UA were 0.01-3 mM and 3.5-10 mM, 2-32 μM and 32-62 μM, and 0.5-1.5 mM and 1.5-3 mM, respectively. All linearity ranges showed excellent correlation coefficients (R^2) equal to or above 0.99.

To perform simultaneous detection of our analytes using composite AuNPs/CQDs/GCE, we varied the concentration of one analyte while the concentrations of the remaining two remained constant. Under the optimized conditions, AA, DA, and UA peak potentials were equal to 0.02, 0.15, and 0.29 V, respectively, and remained almost the same as concentration of one analyte was changed. Under the presence of two other analytes, the peak currents of the detected substance increased linearly as its concentration was increased (see Fig. 6). The linearity ranges of individual analyte detection under the presence of the other two analytes were 0.1-6 mM for AA, 12-27μM and 30-67μM for DA, and 0.34-4 mM for UA. All linearity ranges showed excellent correlation coefficients (R^2) equal to or above 0.99. These linearity ranges were remarkably close to those obtained when only one analyte was present in the solution (see Table 1). Thus, no interference among DA, AA, and UA occurred during their simultaneous electrochemical detection using AuNPs/CQDs/GCE.

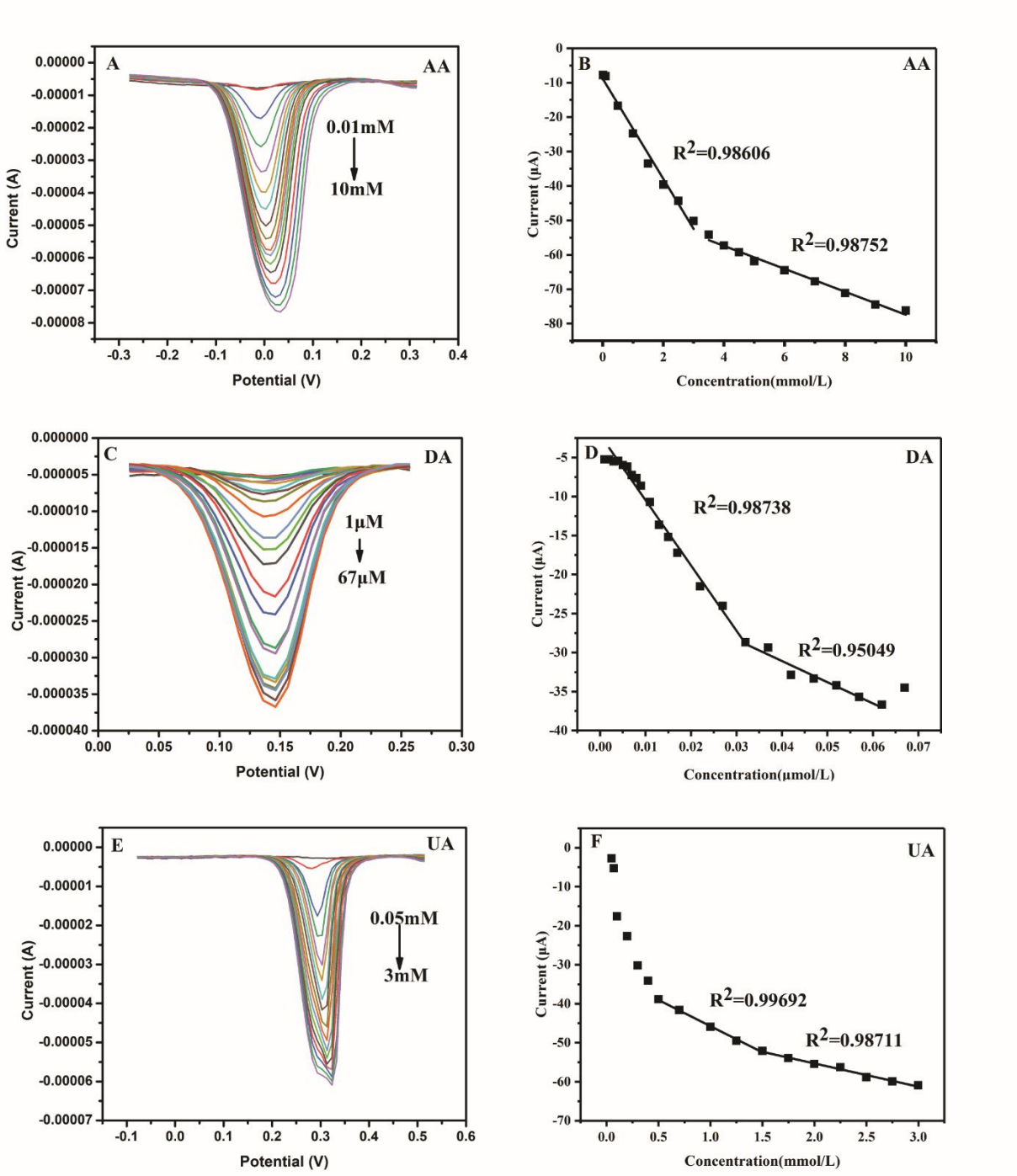

Figure 5. DPV curves (A, C and E) of AuNPs/CQDs/GCE recorded in 0.1 M PBS for individual detection of 0.01-10 mM AA, 1-67 μM DA, and 0.05-3 mM UA. Calibration curves (B, D and F) used I_p plotted as a function of the analyte content.

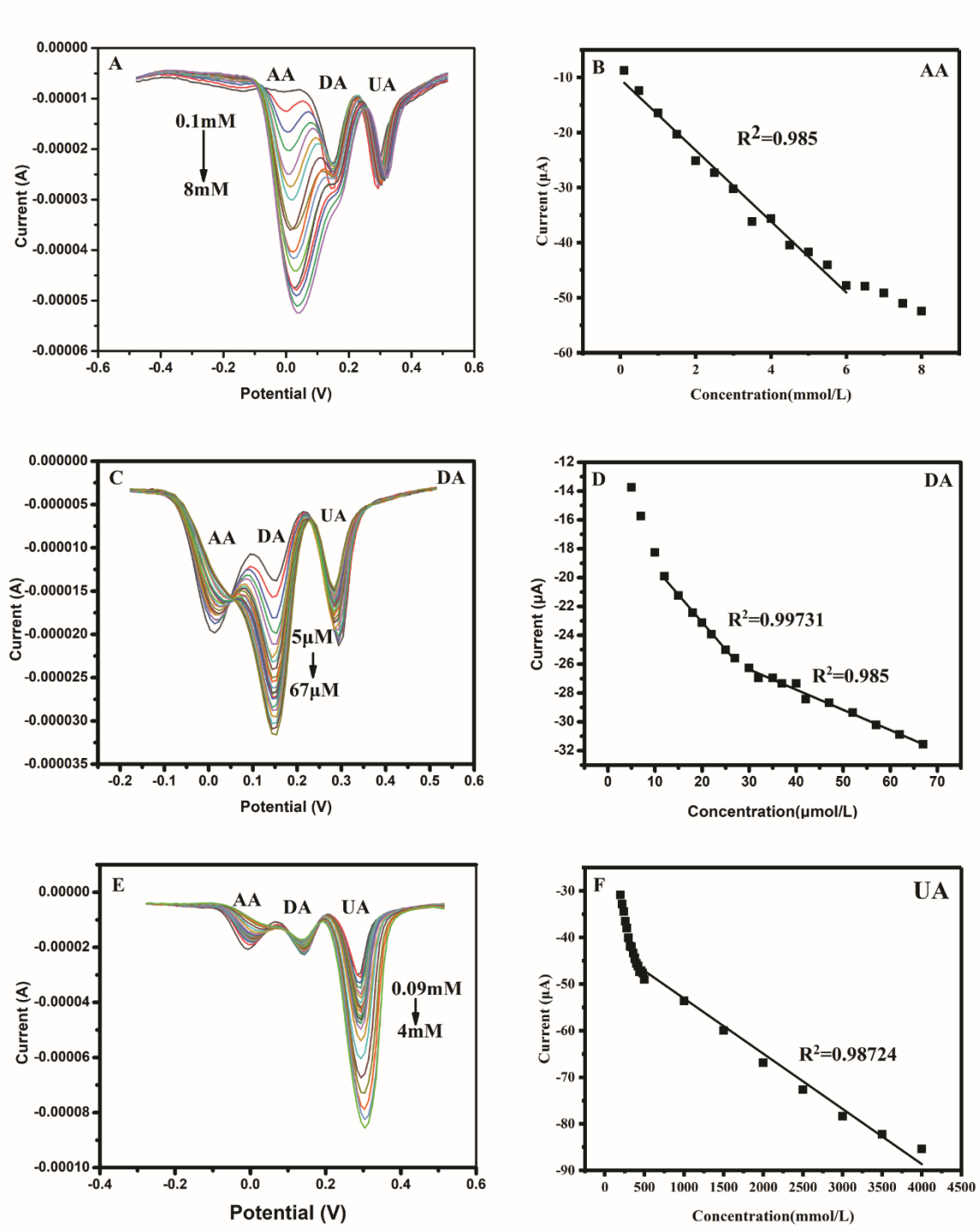

Figure 6. DPV curves of AuNPs/CQDs/GCE recorded in 0.1 M PBS containing: (a) 0.2 mM UA, 20μM DA and 0.1-8 mM AA, (b) 1.5 mM AA, 0.15 mM UA and 5-67 μM DA, and (c) 1.5 mM AA, 15 μM DA and 0.09-4 Mm UA.

Simultaneous electrochemical detection of our analytes showed three well-defined and resolved DPV peaks (see Fig. 7), confirming the excellent performance of our composite AuNPs/CQDs/GCE as an electrochemical sensor. The AuNPs/CQDs/GCE separated the voltammetric signals AA-DA and DA-UA pairs by 150 and 130 mV, respectively. Under the optimized conditions, all peak currents increased

(and remained stable) as the analyte concentrations rose. The calibration curves were linear in specific ranges (see Fig. 7). Thus, AuNPs/CQDs/GCE possessed satisfactory linearity and sensitivity for the simultaneous detection of our analytes.

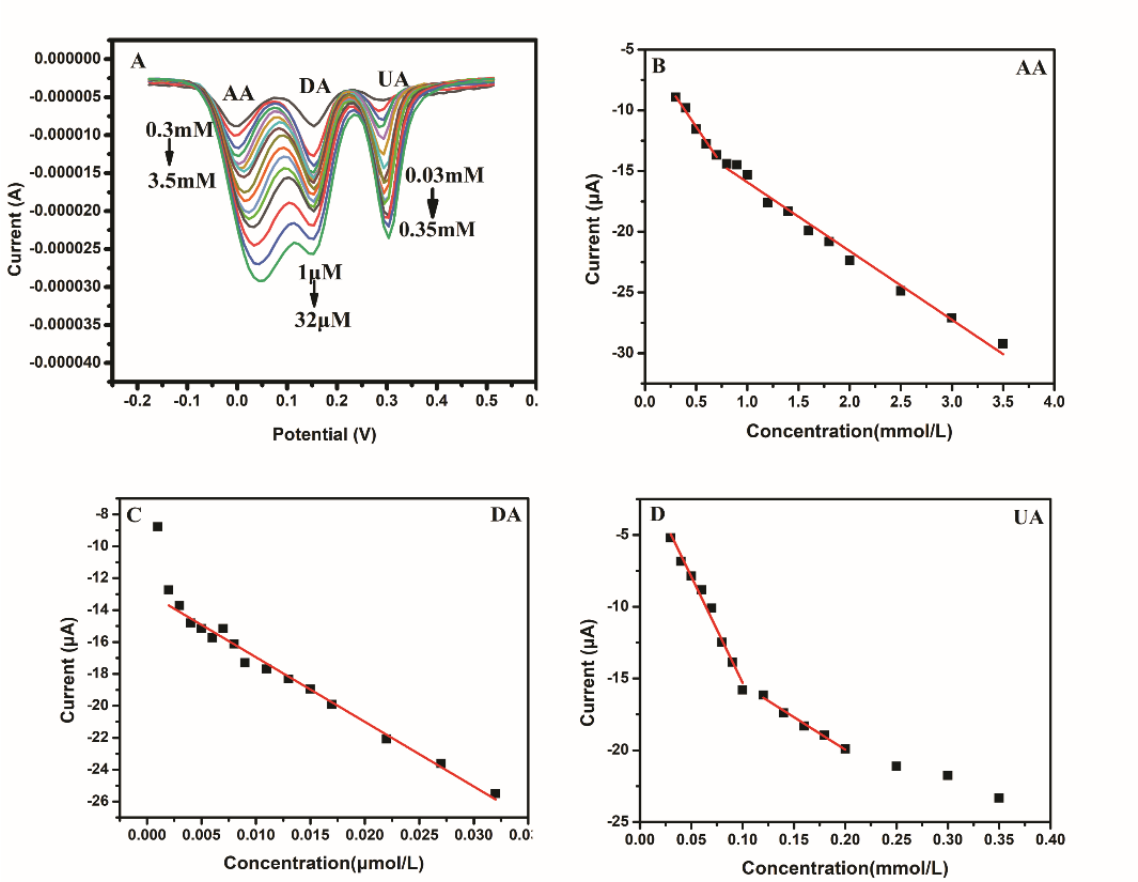

Figure 7. DPV curves (A) and the calibration curves (B-D) for the detection of AA, DA, and UA present at the same time by the AuNPs/CQDs/GCE recorded in 0.1 M PBS. The concentrations of AA, DA, and UA were in the following ranges, restively: 0.3-3.5 mM, 1-32 μM, and 0.03-0.35 mM.

Table 1. Results of the AA, DA, and UA detection by AuNPs/CQDs/GCE. [a] detection of individual analytes; [b] detection of simultaneously present analytes.

Analyte	Linear response range (μM) [a]	Linear regression equation [a]	Linear response range (μM) [b]	Linear regression equation [b]
AA	10-3000	I_{AA} (μA)=-8.85-14.55 C (mM)	300-700	I_{AA} (μA)=-5.131-12.45 C (mM)
	3500-10000	I_{AA} (μA)=-44.07-3.34 C (mM)	800-3500	I_{AA} (μA)=-10.26-5.66 C (mM)
DA	2-32	I_{DA} (μA)=-2.46-817.45 C (μM)	2-32	I_{DA} (μA)=-12.9-405.13 C (μM)
	32-62	I_{DA} (μA)=-20.21-271.86 C (μM)		
UA	500-1500	I_{UA} (μA)=-32.34-13.41 C (mM)	30-100	I_{UA} (μA)=-0.504-147.99 C (mM)
	1500-3000	I_{UA} (μA)=-43.39-5.96 C (mM)	120-200	I_{UA} (μA)=-10.89-43.55 C (mM)

The linearity ranges under the presence of all three analytes were 0.3-0.7 mM and 0.8-3.5 mM for AA, 2-32 μM for DA, 0.03-0.1mM and 0.12-0.2 mM for UA, respectively. All linearity ranges showed excellent correlation coefficients (R^2) equal to or above 0.99. The corresponding electrode sensitivity values in these ranges were 12.45 and 5.66 μA/mM for AA, 405.13 μA/μM for DA, and

147.99 and 43.55 μA/mM for UA (see Table 1). Such excellent sensitivity and activity of our composite AuNPs/CQDs/GCE towards AA, DA and UA detection was ascribed to its large surface area, excellent catalytic oxidative activity as well as high conductivity provided by the synergetic effect of AuNPs and CQDs.

Table 2. AA, DA, and UA detection using electrodes fabricated in this work and reported in the literature.

Modified electrode	Linear response range (μM)			Sensitivity (μA/μM)			Reference
	AA	DA	UA	AA	DA	AA	
SN-GSEC film electrodes	3-1600	0.75-400	0.75-400	0.095 0.071	0.8 0.45	0.68 0.29	[44]
Pd_3Pt_1/PDDA-RGO/GCE	40-1200	4-200	4-400	0.0054	0.0452	0.0352	[45]
Fe_3O_4-SnO_2-Gr/CPE	0.01-23	0.02-2.8	0.015-2.4	1.484	13.082	18.303	[46]
MgO nanobelts/GCE	2.5-15 25-150	0.125-7.5	0.5-3 5-30	0.014 0.002	0.559	0.2 0.068	[47]
SnO_2 /chitosan/GCE	20-220	0.1-18	1-100	0.009	0.196	0.169	[48]
Basic medium/GCE	25-300	3-30	5-70	0.023	0.52	0.19	[49]
ERGO-EBT/AuNPs/GCE	10-900	0.5-20	2-70	0.003	0.164	0.034	[11]
ZnO–Cu_xO–PPy/GCE	200-1000	0.1-130	0.5-70	0.047	0.28	0.33	[50]
Carbon electrode	6-300 300-1500	0.4-20 20-100	1-5 5-250	0.008 0.003	0.573 0.275	0.35 0.151	[51]
AuNPs/CQDs/GCE	300-700 800-3500	2-32	30-100 120-200	0.012 0.0057	405.13	0.148 0.044	This work

Table 2 compares the analytical performances of the electrode fabricated in this work with those reported in the literature. Our AuNPs/CQDs/GCE demonstrated excellent linear response range and sensitivity for the simultaneous AA, DA, and UA detection. Thus, this novel composite electrode can indeed be used for the relevant practical applications.

3.8. Reproducibility and stability

The repeatability of our sensors was evaluated by recording their DPV curves under the presence of AA, DA, and UA using the same electrode. The relative standard deviations (RSD) of five AA, DA, and UA detection tests were equal to 2.9%, 4.7%, and 3.8%, respectively. The reproducibility tests, which were checked using six different composite electrodes, showed that the RSD of the AA, DA, and UA oxidation peak currents were equal to 1.51%, 4.09%, and 1.66%, respectively.

The sensor stability upon storage was examined in relationship to 1mM AA, 15 μM DA, and 0.5 mM UA solutions. After each measurement, the modified electrode was rinsed with PBS and kept at 4 ℃ for ten days. The current losses observed in the DPV curves recorded under the AA, DA, and UA presence were equal to 5%, 11%, and 9%, respectively. After 20 days of storage, the electrode showed the current response towards AA, DA, and UA equal to 78%, 70%, and 73% of the initial performance.

Thus, our composite AuNPs/CQDs/GCE exhibited satisfactory repeatability, stability, and reproducibility.

3.9. Interference study

To assess the selectivity of the AuNPs/CQDs/GCE towards AA, DA, and UA, their presence was tested under the presence of other chemicals. The selectivity of the AuNPs/CQDs/GCE towards 1 mM AA, 80 μM DA and 5 mM UA, assessed under the presence of 100 mM of Na^+, Cl^-, Mg^{2+}, SO_4^{2-}, and glucose, showed that the relative error of the DPV response under the presence of the interfering substances was within ± 5%. Thus, AuNPs/CQDs/GCE demonstrated excellent selectivity towards AA, DA, and UA.

4. CONCLUSIONS

This work reported the fabrication of AuNPs/CQDs-modified glassy carbon electrode (GCE) to detect the presence of ascorbic acid, dopamine as well as uric acid (AA, DA, and UA, respectively). First, CQDs were synthesized using a microwave-assisted method, after which, together with the gold nanoparticles (AuNPs), they were electrodeposited on a GCE. High surface area and excellent electron transport properties of the resulting composite electrode were tested during the electrochemical analysis of AA, DA, and UA presence. During the analysis of the AA, DA, and UA mixture, three well-defined anodic current peaks at 0.02, 0.16, and 0.3 V were distinguished. The composite AuNPs/CQDs/GCE also showed excellent stability, reproducibility, and no interference from the common ions and molecules. Therefore, we strongly believe that this novel AuNPs/CQDs-modified electrode is an excellent platform for electroanalytical sensing and clinical detection applications.

ACKNOWLEDGMENTS
Financial supports from the National Natural Science Foundation of China (Grant No. 81973944 and 81704146) and the National S&T Major Project (No.2018ZX09201011) are acknowledged.

References

1. H. Li, Y. Wang, D. Ye, J. Luo, B. Su, S. Zhang and J. Kong, *Talanta*, 127 (2014) 255.
2. Y.L. Jiang, B.X. Wang, F.D. Meng, Y.X. Cheng and C.J. Zhu, *J. Colloid Interf. Sci.*, 452 (2015) 199.
3. L. Wang, C.C. Gong, Y. Shen, W.H. Ye, M.L. Xu and Y.H. Song, *Sensor. Actuat. B-Chem.*, 242 (2017) 625.
4. B.Kaur, B. Satpatib and R. Srivastava, *New J. Chem.*, 39 (2015) 1115.
5. W. Shen, Y. Zhuo, Y. Chai and R. Yuan, *Anal. Chem.*, 87 (2015) 11345.
6. J.W. Dalley and J.P. Roiser, *Neurosci.*, 215 (2012) 42.
7. B.J. Venton and R.M. Wightman, *Anal.Chem.*, 75 (2003) 414.
8. E.E. Ferapontova, *Electrochim. Acta*, 245 (2017) 664.

9. F.A. Zucca, S. Segura-Aguilar, E. Ferrari, P. Munoz, I. Paris, D. Sulzer, T. Sarna, L. Casella and L. Zecca, *Prog. Neurobio.*, 155 (2017) 96.
10. J. Du, J.J. Cullen and G.R. Buettner, *BBA-Rev. Cancer*, 1826 (2012) 443.
11. N. Alshik, J. Abdullah, S. Kamaruzaman, M. Saiman and Y. Sulaiman, *Arab. J. Chem.*, 11 (2018) 1301.
12. H. Li, Y. Wang, D. Ye, J. Luo, B. Su, S. Zhang and J. Kong, *Talanta*, 127 (2014) 255.
13. Y. Peng, D. Zhang and C. Zhang, *Anal. Methods*, 6 (2014) 8965.
14. L.Q. Yang, N. Huang, Q.J. Lu, M.L. Liu, H.T. Li, Y.Y. Zhang and S.Z. Yao, *Anal. Chim. Acta* 903 (2016) 69.
15. D. Feng, L. Li, X. Han, X. Fang, X. Li and Y. Zhang, *Sens. Actuators B Chem.*, 201 (2014) 360.
16. X.Y. Li, X.J. Lu and X.W. Kan, *J. Electroanal. Chem.*, 799 (2017) 451.
17. G. Muthusankar, A. Sangili, S.M. Chen, R. Karkuzhali, M. Sethupathi, G. Gopu, S. Karthick, R. K. Devi and N. Sengottuvelan, *J. Mol. Liq.*, 268 (2018) 471.
18. X.Y. Xu, R. Ray, Y.L. Gu, H.J. Ploehn, L. Gearheart, K. Raker and W.A. Scrivens, *J. Am. Chem. Soc.*, 126 (2004) 12736.
19. J.H. Shen, Y.H. Zhu, X.L. Yang and C.Z. Li, *Chem. Commun.*, 48 (2012) 3686.
20. R.M. Shereema, T. P. Rao, V.B. S. Kumar, T.V. Sruthi, R. Vishnu, G.R.D. Prabhu and S.S. Shankar, *Mat. Sci. Eng. C Mater.*, 93 (2018) 21.
21. S.Y. Lim, W. Shen and Z.Q. Gao, Chem. *Soc. Rev.*, 44 (2015) 362.
22. X. Wang, L. Cao, F. Lu, M.J. Meziani, H. Li, G. Qi, B. Zhou, B.A. Harruff, F. Kermarrec and Y.P. Sun, *Chem. Commun.*, 25 (2009) 3774.
23. J. Jia, B. Lin, Y. Gao, Y. Jiao, L. Li, C. Dong and S. Shuang, *Spectrochim. Acta*, 211 (2019) 363.
24. S.K. Kailasa, S. Ha, S.H. Baek, L.M.T. Phan, S. Kim, K. Kwak and T.J. Park, *Mater. Sci. Eng. C*, 98 (2019) 834.
25. H. He, X. Zheng, S. Liu, M. Zheng, Z. Xie, Y. Wang, M. Yu and X. Shuai, *Nanoscale*, 10 (2018) 10991.
26. Y. Li, X. Zhang, M. Zheng, S. Liu and Z. Xie, *RSC Adv.*, 6 (2016) 54087.
27. L. Qiao, J. Wang, M. Zheng and Z. Xie, Anal. *Methods*, 10 (2018) 1863.
28. M. Zheng, Y. Li, Y. Zhang and Z. Xie, *RSC Adv.*, 6 (2016) 83501.
29. Y.L. Jiang, B.X. Wang, F.D. Meng, Y.X. Cheng and C.J. Zhu, *J. Colloid Interf. Sci.*, 452 (2015) 199.
30. N. Amini, M. Shamsipur, M.B. Gholivand and A. Barati, *Microchem. J.*, 131 (2017) 9.
31. S. Hu, Q. Huang, Y. Lin, W. Chan, H. Zhang, W. Zhang, Z. Guo, X. Bao, J. Shi and A. Hao, *Electrochim. Acta*, 130 (2014) 805.
32. W. Chan, Q. Huang, S. Hu, H. Zhang, W. Zhang, Z. Wang, M. Zhu, P. Dai and L. Huang, *Electrochim. Acta*, 149 (2014) 237.
33. G. Chen, H. Tong, T. Gao, Y. Chen and G. Li, *Anal. Chim. Acta*, 849 (2014) 1.
34. J. Ju and W. Chen, *Anal. Chem.*, 87 (2015) 1903.
35. W.J. Niu, D. Shan, R.H. Zhu, S.Y. Deng, S. Cosnier and X.J. Zhang, *Carbon*, 96 (2016) 1034.
36. C. Zhao, Y. Jiao, F. Hu and Y. Yang, *Spectrochim. Acta A*, 190 (2018) 360.
37. H. Zhu, X. Wang, Y. Li, Z. Wang, F. Yang and X. Yang, *Chem. Commun.*, 34 (2009) 5118.
38. Y.Y. Wei, D. Zhang, Y.X. Fang, H. Whang, Y.Y. Liu, Z.F. Xu, S.J. Wang and Y. Guo, *J. Sensors*, 2019 (2019) 1.
39. Z.H. Sheng, X.Q. Zheng, J.Y. Xu, W.J. Bao, F.B. Wang and X.H. Xia, *Biosens. Bioelectron.*, 34 (2012) 125.
40. C. Zou, J. Zhong, S. Li, H. Whang, J. Wang, B. Yan and Y. Du, *J. Electroanal. Chem.*, 805 (2017) 110.
41. B.B. Yang, J. Wang, D. Bin, M.S. Zhu, P. Yang and Y.K. Du, *J. Mater. Chem. B*, 3 (2015) 7440.
42. F.A. Harraz, M. Faisal, A.A. Ismail, S.A. Al-sayari, A.E. Al-Salami, A. Al-Hajry and M.S. Al-Assiri, *J. Electroanal. Chem.*, 832 (2019) 225.

43. P.L. Dos Santos, V. Katic, K.C.F. Toledo and J.A. Bonacin, *Sens. Actuators B Chem.*, 255 (2018) 2437.
44. L.L. Huang, Y.Y. Cao and D.F. Diao, *Sens. Actuators B Chem.*, 283 (2019) 556.
45. J. Yan, S. Liu, Z.Q. Zhang, G.W. He, P. Zhou, H.Y. Liang, L.L. Tian, X.M. Zhou and H.J. Jiang, *Colloid. Surface. B*, 111 (2013) 392.
46. H. Bagheri, N. Pajooheshpour, B. Jamali, S. Amidi, A. Hajian and H. Khoshsafar, *Microchem. J.*, 131 (2017) 120.
47. M. Li, W. Guo, H. Li, W. Dai and B. Yang, *Sens. Actuators B Chem.*, 204 (2014) 629.
48. S. Selvarajan, A. Suganthi and M. Rajarajan, *Surf. Interf.*, 7 (2017) 146.
49. Z. Temocin, *Sens. Actuators B Chem.*, 176 (2013) 796.
50. K. Ghanbari and N. Hajheidari, *Anal. Biochem.*, 473 (2015) 53.
51. L.P. Sun, H.J. Li, M.J. Li, C.P. Li, P. Li and B.H. Yang, *J. Electroanal. Chem.*, 783 (2016) 167.

© 2020 The Authors. Published by ESG (www.electrochemsci.org). This article is an open access article distributed under the terms and conditions of the Creative Commons Attribution license (http://creativecommons.org/licenses/by/4.0/).